Chemical Reactivity of Dihydropyrazine Derivatives.　Cycloaddition Behavior toward Ketenes

Kazuhide Nakahara, Koki Yamaguchi, Yasuyuki Yoshitake, Tadatoshi Yamaguchi, and Kazunobu Harano*

Faculty of Pharmaceutical Sciences, Sojo University; 4–22–1 Ikeda, Kumamoto 860–0082, Japan.
Received April 9, 2009; accepted May 7, 2009; published online May 12, 2009

The cycloaddition behavior of dihydropyrazines toward ketenes was investigated using single-crystal X-ray structures of the cycloadducts and density functional theory (DFT) calculation data. The reaction proceeds *via* a stepwise pathway involving an orientation complex prior to formation of the betaine intermediate. This is followed by electrocyclization to afford the 1 : 1 and 1 : 2 adducts bearing *β*-lactam ring(s).

Key words　dihydropyrazine; ketene; imine; cycloaddition; density functional theory; X-ray analysis

Dihydropyrazines (DHPs), which are derived from amino-sugars, exhibit various properties such as specific DNA strand-breakage activity,[1—3] facile dimerization,[4—6] unique ESR spectral behavior,[7—9] *in vitro*, induction of apoptosis[10] and mutagenesis[11,12] *in vivo*. It is thought that all these phenomena originate from the two natural characteristics of DHPs, *i.e.*, their high chemical reactivity and radical generation ability.[4—9]

As exemplified in Chart 1, less substituted DHPs such as 5,6-dimethyl-2,3-dihydropyrazine exhibit high chemical reactivity and readily transform to dimeric heterocyclic compounds *via* aldol condensation or pericyclic ene reaction (Chart 1).[5,6]

In order to clarify the inherent chemical reactivity of DHPs, we studied the cycloaddition behavior of DHPs as diazadienes or imines towards ketenes. The results are discussed in detail on the basis of molecular orbital (MO) calculations on the cycloaddition pathways and the single crystal X-ray analyses of the cycloadducts.

Results and Discussion

First, reactions of relatively stable 2,3-diphenyl DHP derivatives (**1a**—**c**)[13] with ketenes (**2a**—**c**) were performed (Chart 2).

The reaction of **1a** with **2a** provided the 1 : 1 adduct (**3aa**) and two stereoisomeric 1:2 adducts (*anti* **4aa** and *syn* **4aa**). The yields and product ratios for the reactions with **1a**—**c** and **2a**—**c** are summarized in Table 1.
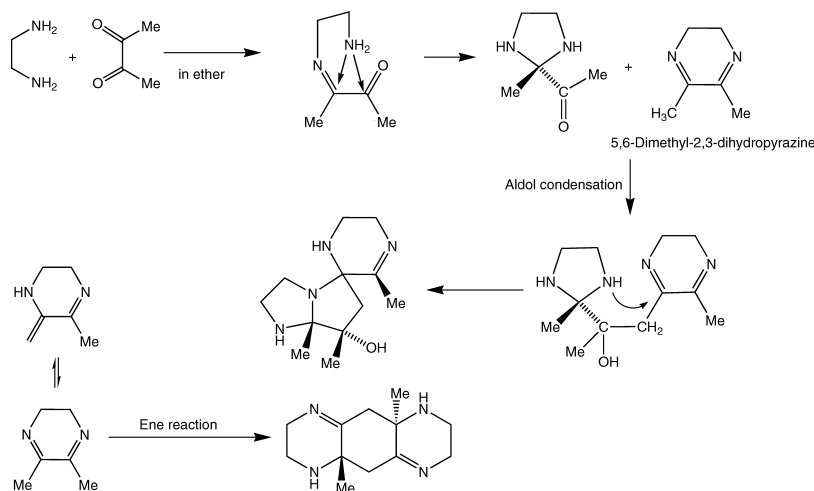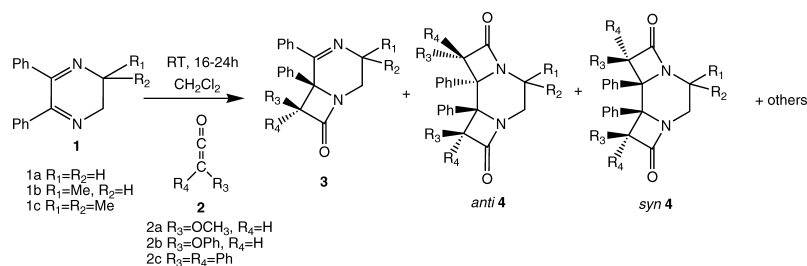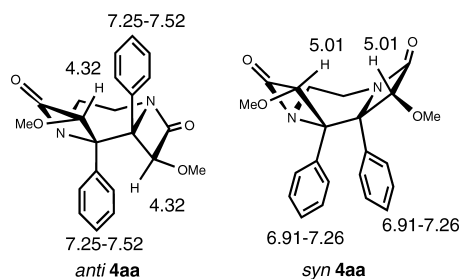

Chart 1

Chart 2

Fig. 1. 500 MHz ^{1}H-NMR Spectral Data for 1 : 2 Adducts

Table 1. Reaction Product (%) and Ratio (*anti* **4** : *syn* **4**) for Dihydropyrazine (**1**) with Ketene (**2**)

Starting substance		Product (%)		Product ratio	Reaction time
		3	**4**	(*anti* **4** : *syn* **4**)	
1a	**2a**	40.1 (**3aa**)	52.6 (**4aa**)	3 : 2	21.5 h
	2b	—	90.2 (**4ab**)	7 : 2	24 h
	2c	90.3 (**3ac**)	—	—	18 h
1b	**2a**	2.3$^{a)}$ (**3ba**)	36.7$^{a)}$ (**4ba**)	—	17 h
	2b	21.5 (**3bb**)	58.6$^{a)}$ (**4bb**)	—	24 h
	2c	33.3 (**3bc**)	—	—	17 h
1c	**2a**	38.8 (**3ca**)	30.2 (**4ca**)	2 : 1	16 h
	2b	42.5 (**3cb**)	54.9 (**4cb**)	5 : 1	24 h
	2c	79.3 (**3cc**)	—	—	22 h

a) Mixture of stereoisomers.

The structures of the adducts were established by MS, IR and NMR spectral data, showing the formation of a *β*-lactam ring. The ^{1}H-NMR spectrum of **3aa** exhibited a methoxy signal at 3.50 ppm, methylene signals at 3.21—4.17 ppm, a methine signal at 4.63 ppm and aromatic proton signals at 7.34—7.85 ppm. The ^{13}C-NMR spectrum exhibited seven non-aromatic carbon signals, suggesting the presence of one methyl (δ 59.3), two methylenes (δ 37.0, 45.2), one methine (δ 89.1), one quaternary (δ 63.7) and two sp^2 carbons (δ 168.4, 171.0). The IR spectrum showed the characteristic absorption of a *β*-lactam carbonyl at 1769 cm^{-1}. The structure of the adduct (**3aa**) was confirmed by comparison of the spectral features with those of the analogous 1 : 1 adducts (**3ba**, **3ac**) whose structures were firmly established by single crystal X-ray analysis (see Fig. 2, Table 2).

Both 1 : 2 adducts showed similar spectral behaviors as observed in the 1 : 1 adducts. Comparison of the ^{1}H-NMR spectra of the 1 : 2 adducts afforded a clue to the determination of the *syn*/*anti* orientation. In the *syn* orientation, the two phenyl rings are in a face-to-face disposition which agrees with the observation that the phenyl hydrogens are shifted upfield (6.91—7.26 ppm) in comparison with those of the *anti* adduct (7.25—7.52 ppm), whereas the methine proton [>CH(OMe)–CO–] of the *anti* adduct resonates at *ca.* 0.7 ppm higher field than that of the *syn* adduct. The assignment of the ^{1}H-NMR spectra of the 1 : 2 adducts (*anti* **4aa** and *syn* **4aa**) is shown in Fig. 1. The structure of *syn* **4aa** was confirmed by single crystal X-ray analysis (see Fig. 2, Table 2).

It is noted that the reaction of **1a**—**c** with diphenylketene (**2c**) gave only the 1 : 1 adduct. The reaction of the monomethyl-substituted DHP (**1b**) with **2a**—**c** gave mixtures of the stereoisomeric cycloadducts. Even in the reaction of **1b**
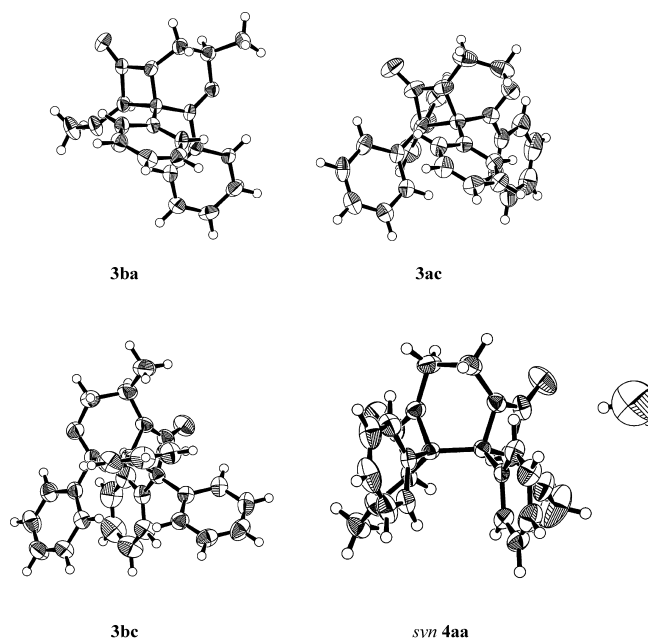

Fig. 2. ORTEP Drawings of the Cycloadducts (**3ba**, **3ac**, **3bc**, *syn* **4aa**)

Table 2. Crystal and Analysis Data for the Adducts

| Crystal data	**3ba**	**3ac**	**3bc**	*syn* **4aa**
Formula	$C_{20}H_{20}N_2O_2$	$C_{30}H_{24}N_2O$	$C_{31}H_{26}N_2O$	$C_{22}H_{24}N_2O_5$
Crystal system	Monoclinic	Monoclinic	Monoclinic	Orthorhombic
Lattice parameters				
a (Å)	19.243(7)	11.656(5)	11.930(3)	14.549(5)
b (Å)	8.149(4)	17.754(7)	18.068(7)	19.032(5)
c (Å)	10.861(3)	10.810(3)	10.863(3)	14.218(5)
β (°)	99.00	90.99(3)	94.09(2)	
V (Å^3)	1682(1)	2236(1)	2335(1)	3937(2)
Space group	$P2_1/n$	$P2_1/n$	$P2_1/n$	$Pbca$
Z	4	4	4	8
Density (calcd.)	1.265	1.272	1.259	1.338
Density (obsd.)	1.266	1.272	1.258	1.335
Unique data used	3868	5117	5347	4526
R	0.095	0.083	0.088	0.072
Rw	0.166	0.108	0.089	0.116
Goodness of fit	1.000	1.001	1.270	1.002
CCDC number	717626	717627	717628	717629

with **2c**, four isomers were recognized, indicating that the reaction was affected by site selectivity in addition to the steric effect. Of those, the structure of **3bc** was established by X-ray analysis (see Fig. 2, Table 2).

The ketene cycloaddition reaction has attracted much attention from both synthetic and theoretical chemists because the [2+2] cycloaddition products of cyclic dienes and ketenes are known to be formed *via* [3,3]-sigmatropic rearrangement of the [4+2] cycloadduct in which the carbonyl double bond of the ketene acts as a dienophile (Chart 3, entry b). This finding has caused a revolution in ketene chemistry.[14]

In this connection, we previously reported another cycloaddition mechanism for the reaction of dihydropyridines with ketenes on the basis of MO calculations,[15] in which the lactam ring formation does not proceed *via* a sequential pericyclic reaction mechanism but takes place by a stepwise reaction mechanism (Chart 3, entry c).

Based on the results for dihydropyridines, we considered that the reaction of a ketene with an α,β-unsaturated cyclic imine does not fall into the new category but involves initial nucleophilic attack of the imine nitrogen on the ketene sp-hybridized carbon, followed by 4π electrocyclic ring closure to give the [2+2] cycloaddition product. This reaction behavior is easily explained by frontier molecular orbital (FMO) theory.[16,17] The highest occupied molecular orbital (HOMO) of the dihydropyridine localizes on the lone pair of the nitrogen atom, 0.35 eV higher than π-NHOMO, and the resulting azadiene readily undergoes conrotatory electrocyclic ring closure (Chart 4).

To confirm the reaction mechanism for the reaction of DHP and ketene, we calculated possible transition-state (TS) structures using the density functional theory (DFT) method at the B3LYP/6-31G (d) level.[18] The TS geometries of [4+2] cycloadditions using parent molecules [DHP as 4π diene towards ketene (C=C or C=O) as 2π dienophile], the interacting bond distances and energies (Hartree) are depicted in Fig. 3. As shown in Fig. 3, [4+2] cycloadditions are energetically
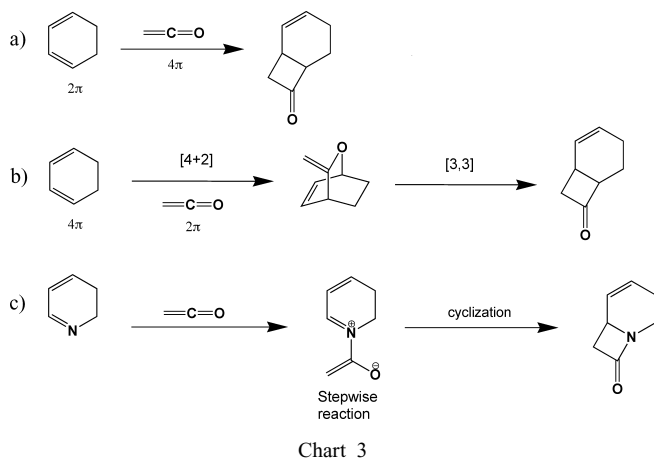
unfavorable[19] in comparison with the reaction barrier for the intermediate formation in the stepwise cyclization reaction (see also Fig. 4).

The energy profile for the model reaction of **1** with **2** is depicted in Fig. 4. The reaction is found to proceed *via* a betaine intermediate followed by electrocyclization.

The energy profile for the reaction of **1a** with **2a** is depicted in Fig. 5. The betaine intermediate is more stable than that for the model reaction using the parent molecules.

The 1:2 cycloadduct formation pathway is also calculated (Fig. 6). The energy profile is essentially the same as that for 1:1 cycloadduct formation. The calculations indicate that the *syn* approach of the methoxy group with respect to the lactam ring is energetically favorable, inconsistent with the experimental results. Close inspection of the reaction pathway between GS and TS1 suggests the presence of an orientation complex (OC)[20—25] in which the reactants loosely combine with each other as compared with the intermediate (IM). The calculation indicates that the *syn* OC is more stable than the *anti* OC. The reaction barrier based on the *anti* OC is lower than that for the *syn* OC, implying dominant formation of the *anti* adduct.

Chart 3

TS-DA$_{C=O}$
53.59 kcal/mol
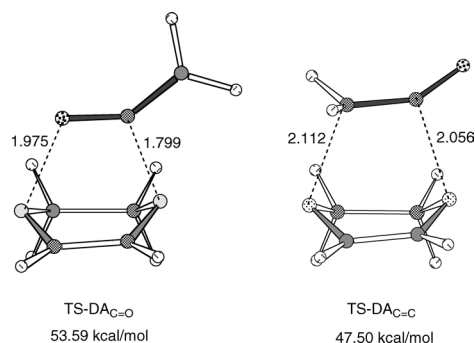
TS-DA$_{C=C}$
47.50 kcal/mol

Fig. 3. B3LYP/6-31G (d) Calculated Transition Structures for Possible [4+2]π Cycloadditions
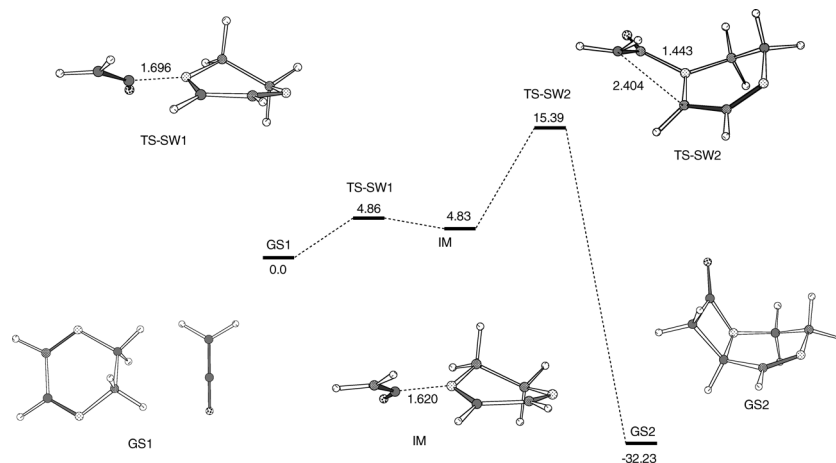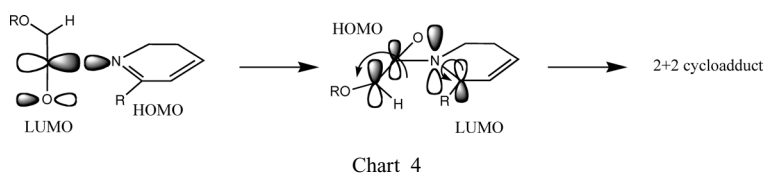

Chart 4

Fig. 4. B3LYP/6-31G (d) Simulation for Model Reaction Pathway for DHP and Ketene Using Parent Addends
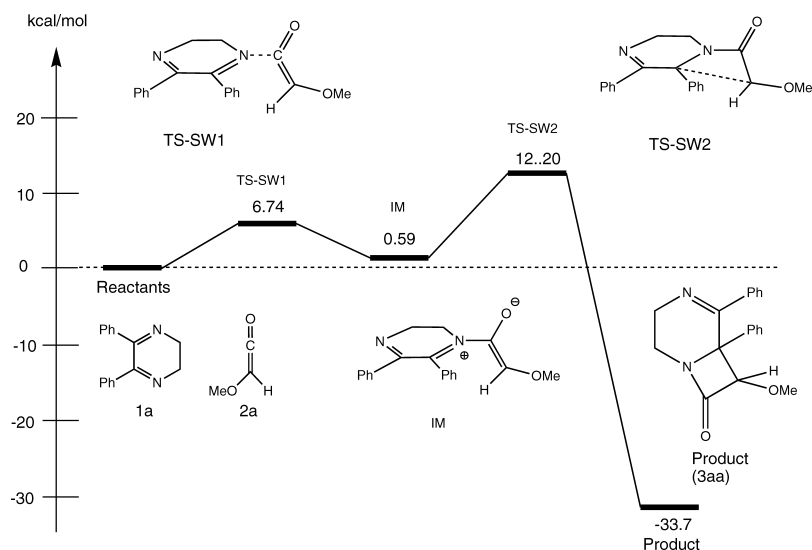
Fig. 5. Reaction Profile for Cycloaddition of **1a** with **2a** Calculated by the B3LYP/6-31G (d) Method
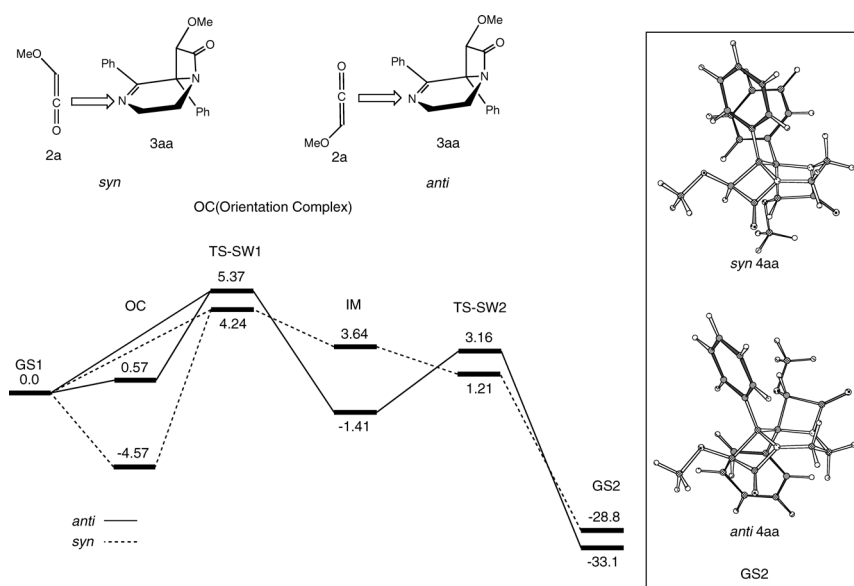
Fig. 6. Energy Diagram for the Reaction of **2a** and **3aa**
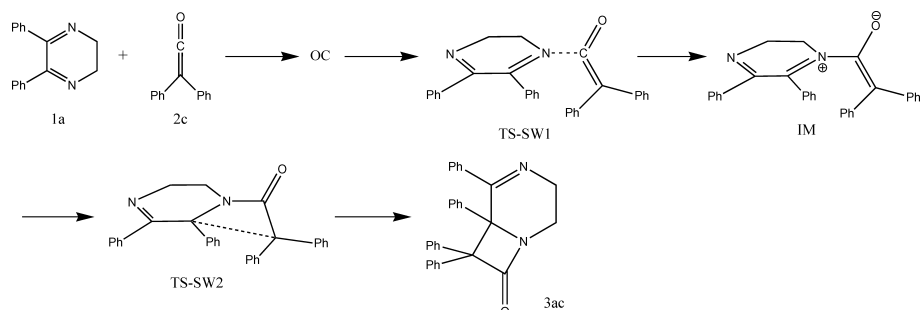
Fig. 7. Possible OC and IM in the Reaction of **1a** with **2c** Used for the MOS-F CNDO/S Calculation

The reaction barrier of the electrocyclization process is lower than that for 1 : 1 adduct formation. This may be due to the difference in the stabilization energy between the ground states of the reactants.

As the reaction may take place in part *via* direct cycloaddition without the OC formation, the product ratio does not necessarily correspond to the calculation prediction.

During the course of the cyclization reaction, a change of color in the reaction mixture was observed. The MOS-F CNDO/S calculations[26] suggested the presence of a charge-transfer complex, presumably due to the OC and IM structures (see Fig. 7, Table 3).

Table 3. Calculated Absorption Wavelength and Oscillator Strength

State	Absorption wavelength (nm)	Oscillator strength[a]
OC	373.33	0.00765
TS-SW1	389.26	0.00489
IM	854.75	0.00525
	367.23	0.00657
	355.49	0.00134
TS-SW2	482.42	0.53804

a) MOS-F CNDO/S.

In summary, DHP shows a high cycloaddition reactivity toward ketenes, in which a stepwise reaction takes place *via* nucleophilic attack of the nitrogen lone pair of DHP on the ketene central carbon, followed by electrocyclization of the azadiene.

Experimental

Melting points are uncorrected. The IR spectra were obtained with a Hitachi 270-30 spectrophotometer. ^{1}H- and ^{13}C-NMR spectra were obtained with JEOL JNM-AL 300 (300 MHz) and JNM-A 500 (500 MHz) spectrometers using tetramethylsilane as an internal standard. Mass spectra were obtained using a JMS-DX303HF instrument.

Materials The DHPs (**1a**—**c**) were prepared according to the literature.[1,27] The ketenes (**2a**—**c**) were also synthesized by established methods.[28,29]

General Procedure A solution of methoxyacetyl chloride (0.43 g, 4 mmol) in CH$_2$Cl$_2$ (5.5 ml) was added dropwise to a solution of 2,3-dihydropyrazine derivative (2 mmol) in CH$_2$Cl$_2$ (7.0 ml) containing triethylamine (0.55 ml). After stirring at room temperature overnight, aqueous NaHCO$_3$ was added to neutralize the reaction mixture. The products were extracted with CH$_2$Cl$_2$ three times and dried over anhydrous MgSO$_4$. Evaporation of the solvent gave crude products, which were purified by chromatography on silica gel. Crystallization from *n*-hexane gave pure cycloadducts.

3aa: Colorless prisms. mp 126—128 °C. IR (KBr) cm^{-1}: 1769 (C=O). ^{1}H-NMR (500 MHz; CDCl$_3$) δ: 3.21 (1H, m, CH), 3.35—3.41 (1H, m, CH), 3.46—3.52 (1H, m, CH), 3.50 (3H, s, OCH$_3$), 4.13—4.17 (1H, m, CH), 4.63 (1H, s, CH), 7.34—7.85 (10H, m, aromatic-H). ^{13}C-NMR (125 MHz; CDCl$_3$) δ: 37.0 (C2), 45.2 (C3), 59.3 (C7-OMe), 63.7 (C6), 89.1 (C7), 127.5, 128.3, 128.4, 128.6, 128.7, 130.9, 134.8, 136.0 (aromatic-C), 168.4 (C=N), 171.0 (C=O). EI-MS (*m/z*): 306 (M$^+$+1). *Anal.* Calcd for C$_{19}$H$_{18}$N$_2$O$_2$: C, 74.49; H, 5.92; N, 9.14. Found: C, 74.33; H, 5.70; N, 9.14.

anti **4aa**: Colorless prisms. mp 212—214 °C. IR (KBr) cm^{-1}: 1760 (C=O), 1740 (C=O). ^{1}H-NMR (500 MHz; CDCl$_3$) δ: 3.07 (6H, s, OCH$_3$), 3.44 (2H, d, *J*=7.9 Hz, CH$_2$), 4.10 (2H, d, *J*=7.9 Hz, CH$_2$), 4.32 (2H, s, CH$_2$), 7.40—7.52 (10H, m, aromatic-H). ^{13}C-NMR (125 MHz; CDCl$_3$) δ: 36.6 (C6, C7), 58.2 (C3-OMe, C10-OMe), 71.3 (C1, C2), 90.5 (C3, C10), 127.22, 127.61, 127.75, 127.92, 128.11, 128.51, 137.11 (aromatic-C), 165.69 (C=O). FAB-MS (*m/z*): 379 (M$^+$+1). *Anal.* Calcd for C$_{22}$H$_{22}$N$_2$O$_4$: C, 69.83; H, 5.86; N, 7.40. Found: C, 69.58; H, 5.90; N, 7.22.

syn **4aa**: Colorless prisms. mp 248—251 °C. IR (KBr) cm^{-1}: 1749 (C=O). ^{1}H-NMR (500 MHz; CDCl$_3$) δ: 3.26 (6H, s, OCH$_3$), 3.52 (2H, d, *J*=7.3 Hz, CH$_2$), 4.17 (2H, d, *J*=7.3 Hz, CH$_2$), 5.01 (2H, s, CH), 6.91—7.26 (10H, m, aromatic-H). ^{13}C-NMR (125 MHz; CDCl$_3$) δ: 37.9 (C6, C7), 58.1 (C3-OMe, C10-OMe), 70.7 (C1, C2), 88.0 (C3, C10), 127.62, 127.72, 127.78, 127.93, 136.51 (aromatic-C), 168.97 (C=O). EI-MS (M$^+$). *Anal.* Calcd for C$_{22}$H$_{22}$N$_2$O$_4$: C, 69.83; H, 5.86; N, 7.40. Found: C, 69.95; H, 5.68; N, 7.50.

anti **4ab**: Colorless prisms. mp 222—224 °C. IR (KBr) cm^{-1}: 1760 (C=O). ^{1}H-NMR (500 MHz; CDCl$_3$) δ: 3.56 (2H, d, *J*=7.9 Hz, CH$_2$), 4.20 (2H, d, *J*=7.9 Hz, CH$_2$), 5.11 (2H, s, CH), 6.62—7.40 (20H, m, aromatic-H). ^{13}C-NMR (125 MHz; CDCl$_3$) δ: 36.7 (C6, C7), 71.8 (C1, C2), 87.1 (C3, C10), 116.46, 122.68, 128.68, 128.76, 129.35, 136.37, 156.93 (aromatic-C), 164.9 (C=O). EI-MS (*m/z*): 502 (M$^+$). *Anal.* Calcd for C$_{32}$H$_{26}$N$_2$O$_4$: C, 76.48; H, 5.21; N, 5.57. Found: C, 76.33; H, 5.18; N, 5.59.

syn **4ab**: Colorless prisms. mp 118—120 °C. IR (KBr) cm^{-1}: 1754 (C=O). ^{1}H-NMR (500 MHz; CDCl$_3$) δ: 3.62 (2H, d, *J*=7.3 Hz, CH$_2$), 4.29 (2H, d, *J*=7.3 Hz, CH$_2$), 5.61 (2H, s, CH), 6.91—7.34 (20H, m, aromatic-H). ^{13}C-NMR (125 MHz; CDCl$_3$) δ: 38.1 (C6, C7), 71.2 (C1, C2), 84.7 (C3, C10), 116.4, 123.1, 127.4, 127.9, 128.2, 129.7, 135.9, 157.0 (aromatic-C), 168.0 (C=O). FAB-MS (*m/z*): 503 (M$^+$+1). HR-MS Calcd for C$_{32}$H$_{27}$N$_2$O$_4$

(M$^+$+H): 503.1971. Found: 503.2018.

3ac: Colorless prisms. mp 174—176 °C.[30] IR (KBr) cm^{-1}: 3100—2800 (C–H), 1752 (C=O), 1601 (C=N), 1574, 1495 (Ph), 1446 (C=N). ^{1}H-NMR (500 MHz; CDCl$_3$) δ: 3.22—3.27 (1H, m, CH), 3.47—3.54 (1H, m, CH), 3.91—3.96 (1H, m, CH), 4.27—4.33 (1H, m, CH), 6.79—7.53 (20H, m, aromatic-H). ^{13}C-NMR (125 MHz; CDCl$_3$) δ: 34.8 (C2), 45.8 (C3), 68.9 (C6), 78.6 (C7), 127.0, 127.3, 127.4, 127.7, 127.8, 128.0, 128.3, 128.9, 129.2, 129.6, 135.6, 137.8, 138.2, 138.4 (aromatic-C), 169.84 (C=N), 170.51 (C=O). FAB-MS (*m/z*): 429 (M$^+$+1). *Anal.* Calcd for C$_{30}$H$_{24}$N$_2$O: C, 84.08; H, 5.65; N, 6.54. Found: C, 84.18; H, 5.55; N, 6.54.

3ba: Colorless prisms. mp 189—191 °C. IR (KBr) cm^{-1}: 1750 (C=O). ^{1}H-NMR (500 MHz; CDCl$_3$) δ: 1.29 (3H, d, *J*=7.3 Hz, CH$_3$), 2.55 (1H, dd, *J*=9.1, 13.4 Hz, CH), 3.62 (3H, s, OCH$_3$), 3.86 (1H, dd, *J*=6.7, 13.4 Hz, CH), 4.08—4.12 (1H, m, CH), 4.74 (1H, s, CH), 7.25—7.80 (10H, m, aromatic-H). ^{13}C-NMR (125 MHz; CDCl$_3$) δ: 20.8 (C3-Me), 40.7 (C2), 51.8 (C3), 59.9 (C7-OMe), 61.5 (C6), 90.7 (C7), 127.5, 127.7, 128.0, 128.4, 128.6, 129.8, 130.5, 135.6, 136.2 (aromatic-C), 163.5 (C=N), 166.0 (C=O). EI-MS (*m/z*): 320 (M$^+$). *Anal.* Calcd for C$_{20}$H$_{20}$N$_2$O$_2$: C, 74.98; H, 6.29; N, 8.74. Found: C, 74.97; H, 6.25; N, 8.63.

3ba-1: Recognized as a minor product in the ^{1}H-NMR spectrum of **3ba**. ^{1}H-NMR (300 MHz; CDCl$_3$) δ: 1.78 (3H, d, *J*=6.6 Hz, CH$_3$), 3.29 (3H, s, OCH$_3$), 3.60 (1H, m, CH), 3.92—3.96 (2H, m, CH), 5.03 (1H, s, CH), 6.86—7.25 (10H, m, aromatic-H).

4ba: Colorless prisms. mp 158—160 °C. IR (KBr) cm^{-1}: 1752 (C=O). ^{1}H-NMR (300 MHz; CDCl$_3$) δ: 1.75 (3H, d, *J*=6.7 Hz, CH$_3$), 3.07—3.18 (6H, m, OCH$_3$), 3.09 (1H, s, CH), 3.84 (1H, m, CH), 4.10 (1H, dd, *J*=4.4, 12.8 Hz, CH), 4.19 (1H, s, CH), 4.43 (1H, s, CH), 7.25—7.52 (10H, m, aromatic-H). ^{13}C-NMR (125 MHz; CDCl$_3$) δ: 16.2 (C7-Me), 44.6 (C6), 49.5 (C7), 58.2 (C3-OMe), 58.3 (C10-OMe), 70.5 (C1), 74.2 (C2), 85.5 (C3), 90.5 (C10), 127.0, 127.2, 127.5, 127.7, 127.8, 127.9, 128.0, 128.4, 128.7, 128.8, 129.1, 129.8, 130.5, 137.2, 137.3 (aromatic-C), 165.4 (C=O), 165.7 (C=O). EI-MS (*m/z*): 392 (M$^+$). *Anal.* Calcd for C$_{23}$H$_{24}$N$_2$O$_4$: C, 70.39; H, 6.16; N, 7.14. Found: C, 70.11; H, 6.12; N, 7.10.

4ba-1: Recognized as a minor product in the ^{1}H-NMR spectrum of **4ba**. ^{1}H-NMR (300 MHz; CDCl$_3$) δ: 1.46 (3H, d, *J*= 6.4 Hz, CH$_3$), 3.00—3.09 (1H, m, CH), 3.29 (6H, s, OCH$_3$), 4.05—4.12 (1H, m, CH), 4.18—4.24 (1H, m, CH), 4.90 (1H, s, CH), 4.97 (1H, s, CH), 6.86—7.25 (10H, m, aromatic-H).

3bb: Colorless prisms. mp 164—166 °C. IR (KBr) cm^{-1}: (C=O). ^{1}H-NMR (500 MHz; CDCl$_3$) δ: 1.46—1.47 (3H, s, CH$_3$), 3.16—3.17 (1H, m, CH), 3.30—3.31 (1H, m, CH), 3.51—3.52 (1H, m, CH), 5.30—5.31 (1H, s, CH), 6.94—7.77 (15H, m, aromatic-H). ^{13}C-NMR (125 MHz; CDCl$_3$) δ: 20.9 (CH$_3$), 44.1 (C2), 50.7 (C3), 63.9 (C5), 86.1 (C8), 117.3, 123.0, 127.8, 128.5, 128.8, 129.1, 129.2, 129.6, 131.1, 134.8, 135.7 (aromatic-C), 157.4 (OPh), 167.6 (C=N), 169.5 (C=O). EI-MS (*m/z*): 382 (M$^+$). HR-MS Calcd for C$_{25}$H$_{23}$N$_2$O$_2$(M$^+$+H): 383.1760. Found: 383.1723.

4bb: Colorless prisms. mp 204—205 °C. IR (KBr) cm^{-1}: 1757 (C=O). ^{1}H-NMR (500 MHz; CDCl$_3$) δ: 1.55 (3H, d, *J*=6.7 Hz, CH$_3$), 3.65 (1H, dd, *J*=5.5, 12.8 Hz, CH), 3.87 (1H, dd, *J*=2.4, 12.8 Hz, CH), 4.51—4.54 (1H, m, CH), 5.12 (1H, s, CH), 5.40 (1H, s, CH), 6.56—7.43 (20H, m, aromatic-H). ^{13}C-NMR (125 MHz; CDCl$_3$) δ: 19.3 (C7-Me), 42.6 (C6), 43.5 (C7), 71.3 (C1), 73.7 (C2), 87.0 (C3), 88.3 (C10), 116.7, 122.7, 122.8, 128.2, 128.4, 128.6, 128.7, 128.8, 129.3, 129.4, 136.5, 136.9, 156.9, 157.0 (aromatic-C), 166.2 (C=O), 166.7 (C=O). EI-MS (*m/z*): 516 (M$^+$). *Anal.* Calcd for C$_{33}$H$_{28}$N$_2$O$_4$: C, 76.73; H, 5.46; N, 5.42. Found: C, 76.64; H, 5.26; N, 5.42.

Continued fractional crystallization caused enrichment but the minor products could not be isolated in pure form. The following products were recognized in the ^{1}H-NMR spectrum of the enriched fractions whose structures were determined by comparison of the ^{1}H-NMR data with each other.

4bb-1: ^{1}H-NMR (300 MHz; CDCl$_3$) δ: 1.81 (3H, d, *J*=6.8 Hz, CH$_3$), 3.21—3.29 (1H, m, CH), 3.93—4.00 (1H, m, CH), 4.17—4.22 (1H, m, CH), 5.02 (1H, s, CH), 5.18 (1H, s, CH), 6.55—7.40 (20H, m, aromatic-H).

4bb-2: ^{1}H-NMR (300 MHz; CDCl$_3$) δ: 1.41 (3H, d, *J*=6.6 Hz, CH$_3$), 3.06—3.14 (1H, m, CH), 4.13—4.20 (1H, m, CH), 4.31—4.39 (1H, m, CH), 5.48 (1H, s, CH), 5.55 (1H, s, CH), 6.78—7.31 (20H, m, aromatic-H).

4bb-3: ^{1}H-NMR (300 MHz; CDCl$_3$) δ: 1.84 (3H, d, *J*=6.6 Hz, CH$_3$), 3.70—3.73 (1H, m, CH), 4.01—4.07 (2H, m, CH), 5.61 (1H, s, CH), 5.62 (1H, s, CH), 6.78—7.31 (20H, m, aromatic-H).

3bc: Colorless prisms. mp 184—186 °C. IR (KBr) cm^{-1}: 1747 (C=O). ^{1}H-NMR (500 MHz; CDCl$_3$) δ: 1.29 (3H, d, *J*=6.1 Hz, CH$_3$), 2.79 (1H, dd, *J*=10.9, 14.6 Hz, CH), 4.09—4.14 (1H, m, CH), 4.27 (1H, dd, *J*=6.1, 14.6 Hz, CH), 6.72—7.53 (20H, m, aromatic-H). ^{13}C-NMR (125 MHz; CDCl$_3$) δ: 19.8 (C3-Me), 43.9 (C3), 52.6 (C2), 69.9 (C6), 78.5 (C7), 126.9,

127.3, 127.4, 127.5, 127.7, 127.8, 128.0, 128.2, 128.4, 128.5, 128.9, 129.1, 129.4, 129.5, 135.8, 138.4, 138.8, 138.9 (aromatic-C), 171.92 (C=N), 172.42 (C=O). EI-MS (*m/z*): 442 (M+). *Anal.* Calcd for $C_{32}H_{28}N_2O$: C, 84.13; H, 5.92; N, 6.33. Found: C, 84.17; H, 5.99; N, 6.26.

3ca: Colorless prisms. mp 114—116 °C. IR (KBr) cm^{-1}: 1754 (C=O). ^{1}H-NMR (500 MHz; CDCl$_3$) δ: 1.25 (3H, s, CH$_3$), 1.33 (3H, s, CH$_3$), 2.71 (1H, d, *J*=13.4 Hz, CH), 3.63 (3H, s, OMe), 3.67 (1H, d, *J*=13.4 Hz, CH), 4.72 (1H, s, CH), 7.25—7.82 (10H, m, aromatic-H). ^{13}C-NMR (125 MHz; CDCl$_3$) δ: 28.6 (C3-Me), 30.3 (C3-Me), 45.4 (C2), 55.3 (C3), 59.9 (C7-OMe), 61.3 (C6), 90.7 (C7), 127.6, 128.0, 128.4, 129.8, 130.3, 135.6, 136.3 (aromatic-C), 161.1 (C=N), 166.5 (C=O). EI-MS (*m/z*): 334 (M$^+$+1). *Anal.* Calcd for $C_{21}H_{22}N_2O_2$: C, 75.42; H, 6.63; N, 8.38. Found: C, 75.51; H, 6.67; N, 8.32.

anti **4ca**: Colorless prisms. mp 209—211 °C. IR (KBr) cm^{-1}: 1752 (C=O). ^{1}H-NMR (500 MHz; CDCl$_3$) δ: 1.33 (3H, s, CH$_3$), 1.79 (3H, s, CH$_3$), 2.96 (3H, s, OCH$_3$), 3.19 (3H, s, OCH$_3$), 3.21 (1H, d, *J*=12.8 Hz, CH), 3.82 (1H, d, *J*=12.8 Hz, CH), 4.06 (1H, s, CH), 4.95 (1H, s, CH), 7.38—7.60 (10H, m, aromatic-H). ^{13}C-NMR (125 MHz; CDCl$_3$) δ: 25.3 (C7-Me), 26.5 (C7-Me), 50.0 (C6), 55.2 (C7), 58.1 (C3-OMe), 58.5 (C10-OMe), 69.4 (C1), 73.1 (C2), 89.8 (C3), 90.1 (C10), 128.0, 128.2, 128.4, 128.5, 128.9, 138.0, 138.1 (aromatic-C), 166.7 (C=O), 166.9 (C=O). EI-MS (*m/z*): 406 (M$^+$). *Anal.* Calcd for $C_{24}H_{26}N_2O_4$: C, 70.92; H, 6.45; N, 6.89. Found: C, 70.95; H, 6.49; N, 6.93.

syn **4ca**: Colorless prisms. mp 148—150 °C. IR (KBr) cm^{-1}: 1748 (C=O). ^{1}H-NMR (300 MHz; CDCl$_3$) δ: 0.88 (3H, s, CH$_3$), 1.62 (3H, s, CH$_3$), 2.91 (1H, d, *J*=14.3 Hz, CH), 3.29 (3H, s, OCH$_3$), 3.61 (3H, s, OCH$_3$), 3.76 (1H, d, *J*=14.4 Hz, CH), 4.91 (2H, s, CH), 7.07—7.60 (10H, m, aromatic-H). ^{13}C-NMR (125 MHz; CDCl$_3$) δ: 26.3 (C7-Me), 26.6 (C7-Me), 48.6 (C6), 55.4 (C7), 59.5 (C3-OMe), 59.7 (C10-OMe), 64.5 (C1), 74.1 (C2), 87.2 (C3), 90.4 (C10), 126.4, 127.4, 127.8, 128.1, 128.3, 128.4, 128.6, 128.7, 131.2, 135.6, 138.1 (aromatic-C), 166.2 (C=O), 173.8 (C=O). EI-MS (*m/z*): 406 (M$^+$). HR-MS Calcd for $C_{24}H_{27}N_2O_4$ (M$^+$+H): 407.1971. Found: 407.1982.

3cb: Colorless prisms. mp 113—115 °C. IR (KBr) cm^{-1}: 1769 (C=O). ^{1}H-NMR (500 MHz; CDCl$_3$) δ: 1.26 (3H, s, CH$_3$), 1.37 (3H, s, CH$_3$), 2.76 (1H, d, *J*=13.4 Hz, CH), 3.72 (1H, d, *J*=13.4 Hz, CH), 5.41 (1H, s, CH), 6.99—7.81 (15H, m, aromatic-H). ^{13}C-NMR (125 MHz; CDCl$_3$) δ: 28.5 (C3-Me), 30.3 (C3-Me), 45.5 (C2), 55.3 (C3), 61.2 (C6), 87.0 (C7), 117.2, 123.0, 127.6, 128.0, 128.3, 128.4, 128.5, 129.6, 130.1, 130.4, 135.4, 135.8 (aromatic-C), 157.6 (OPh), 160.6 (C=N), 165.3 (C=O). HR-MS Calcd for $C_{26}H_{25}N_2O_2$ (M$^+$+H): 397.1916. Found: 397.1925.

anti **4cb**: Colorless prisms. mp 193—195 °C. IR (KBr) cm^{-1}: 1753 (C=O). ^{1}H-NMR (500 MHz; CDCl$_3$) δ: 1.43 (3H, s, CH$_3$), 1.85 (3H, s, CH$_3$), 3.29 (1H, d, *J*=12.8 Hz, CH), 3.91 (1H, d, *J*=13.0 Hz, CH), 4.94 (1H, s, CH), 5.58 (1H, s, CH), 6.49—7.50 (20H, m, aromatic-H). ^{13}C-NMR (125 MHz; CDCl$_3$) δ: 25.2 (C7-Me), 26.5 (C7-Me), 50.0 (C6), 55.5 (C7), 69.9 (C1), 73.2 (C2), 87.2 (C3), 87.3 (C10), 116.9, 117.0, 122.6, 122.9, 128.2, 128.3, 128.4, 128.8, 129.1, 129.4, 137.2, 137.7 (aromatic-C), 157.0 (OPh), 157.1 (OPh), 165.9 (C=O), 166.0 (C=O). FAB-MS (*m/z*): 530 (M$^+$). *Anal.* Calcd for $C_{34}H_{30}N_2O_4$: C, 76.96; H, 5.70; N, 5.28. Found: C, 76.81; H, 5.65; N, 5.24.

syn **4cb**: Recognized as a minor product in the ^{1}H-NMR spectrum of *anti* **4cb**. ^{1}H-NMR (500 MHz; CDCl$_3$) δ: 1.64 (3H, s, CH$_3$), 1.71 (3H, s, CH$_3$), 2.99 (1H, d, *J*=14.4 Hz, CH), 3.84 (1H, d, *J*=14.4 Hz, CH), 5.43 (1H, s, CH), 5.54 (1H, s, CH), 6.77—7.81 (20H, m, aromatic-H).

3cc: Colorless prisms. mp 176—178 °C. IR (KBr) cm^{-1}: 1757 (C=O). ^{1}H-NMR (500 MHz; CDCl$_3$) δ: 1.15 (3H, s, CH$_3$), 1.61 (3H, s, CH$_3$), 2.60 (1H, d, *J*=13.5 Hz, CH), 3.93 (1H, d, *J*=13.5 Hz, CH), 6.81—7.54 (20H, m, aromatic-H). ^{13}C-NMR (125 MHz; CDCl$_3$) δ: 29.3 (C3-Me), 30.1 (C3-Me), 44.9 (C2), 55.0 (C3), 66.8 (C6), 78.6 (C7), 127.0, 127.2, 127.3, 127.4, 127.9, 128.2, 128.9, 129.0, 129.7, 130.4, 136.1, 137.3, 137.6, 138.4 (aromatic-C). FAB-MS (*m/z*): 456 (M$^+$). *Anal.* Calcd for $C_{32}H_{28}N_2O$: C, 84.18; H, 6.18; N, 6.14. Found: C, 84.01; H, 6.08; N, 6.11.

Molecular Orbital (MO) Calculations Semi-empirical MO calculations were run through the CS Chem3D Pro interface and WINMOPAC3.5 using MOPAC2002[26)] on an Intel personal computer and iBook Macintosh G4 computer. The *ab initio* and density functional theory (DFT) computations[18)] were carried out on a HIT parallel computer (Itanium 2, 2 node-4 CPU). The AM1-optimized structures or PM5-optimized structures were used as starting geometries for the *ab initio* and DFT calculations. The energies were corrected using zero point vibrational energy (scaled by a factor of 0.9804). The B3LYP/6-31G (d) calculated data are available upon request through e-mail.

Single Crystal X-Ray Analysis of 3ba, 3ac, 3bc and *syn* 4aa The re-flection data were measured on a RIGAKU AFC7R four-circle autodiffractometer with a graphite monochromated Mo*K*α radiation (50 kV–150 mA) and rotating anode generator. The data were collected at a temperature of 23±1 °C to a maximum 2θ value of 55.0°. The structures were solved by direct method (SIR-92),[31)] and hydrogen atoms were placed in the calculation. A full-matrix least-squares technique was used with anisotropic thermal parameters for non-hydrogen atoms and riding model for hydrogen atoms. All calculations were performed using the Crystal Structure[32)] crystallographic software package.

References and Notes
1) Yamaguchi T., Kashige N., Mishiro N., Miake F., Watanabe K., *Biol. Pharm. Bull.*, **19**, 1261—1265 (1996).
2) Kashige N., Yamaguchi T., Mishiro N., Hanazono H., Miake F., Watanabe K., *Biol. Pharm. Bull.*, **18**, 653—658 (1995).
3) Yamaguchi T., Ito S., Kashige N., Nakahara K., Harano K., *Chem. Pharm. Bull.*, **55**, 532—536 (2007).
4) Yamaguchi T., Ito S., Iwase Y., Watanabe K., Harano K., *Heterocycles*, **51**, 2305—2309 (1999).
5) Yamaguchi T., Ito S., Iwase Y., Watanabe K., Harano K., *Heterocycles*, **53**, 1677—1680 (2000).
6) Yamaguchi T., Eto M., Harano K., Kashige N., Watanabe K., Ito S., *Tetrahedron*, **55**, 675—686 (1999).
7) Yamaguchi T., Matsumoto S., Watanabe K., *Tetrahedron Lett.*, **39**, 8311—8312 (1998).
8) Kashige N., Takeuchi T., Matsumoto S., Takechi S., Miake F., Yamaguchi T., *Biol. Pharm. Bull.*, **28**, 419—423 (2005).
9) Takeda O., Takechi S., Ito S., Omori H., Katoh T., Yamaguchi T., *Biol. Pharm. Bull.*, **30**, 1663—1667 (2007).
10) Yamaguchi T., Nomura H., Matsunaga K., Ito S., Takata J., Karube Y., *Biol. Pharm. Bull.*, **26**, 1523—1527 (2003).
11) Takechi S., Yamaguchi T., Nomura H., Minematsu T., Nakayama T., *Mutat. Res.*, **560**, 49—55 (2004).
12) Takechi S., Yamaguchi T., Nomura H., Minematsu T., Adachi M., Kurata H., Kurata R., *Biol. Pharm. Bull.*, **29**, 17—20 (2006).
13) Sakamoto M., Kawasaki T., Ishii K., Tamura O., *Yakugaku Zasshi*, **123**, 717—759 (2003).
14) Machiguchi T., Hasegawa T., Ishiwata A., Terashima S., Yamabe S., Minato T., *J. Am. Chem. Soc.*, **121**, 4771—4786 (1999).
15) Oiso S., Eto M., Yoshitake Y., Harano K., *Chem. Pharm. Bull.*, **51**, 1068—1074 (2003).
16) Fukui K., "Kagaku Hanno to Densi no Kido (Chemical Reactions and Electron Orbitals)," Maruzen, Tokyo, 1976.
17) Fleming I., "Frontier Orbitals and Organic Chemical Reactions," Wiley, London, 1976.
18) Gaussian 98, Revision A.7. Frisch M. J., Trucks G. W., Schlegel H. B., Scuseria G. E., Robb M. A., Cheeseman J. R., Montgomery J. A. Jr., Vreven T., Kudin K. N., Burant J. C., Millam J. M., Iyengar S. S., Tomasi J., Barone V., Mennucci B., Cossi M., Scalmani G., Rega N., Petersson G. A., Nakatsuji H., Hada M., Ehara M., Toyota K., Fukuda R., Hasegawa J., Ishida M., Nakajima T., Honda Y., Kitao O., Nakai H., Klene M., Li X., Knox J. E., Hratchian H. P., Cross J. B., Bakken V., Adamo C., Jaramillo J., Gomperts R., Stratmann R. E., Yazyev O., Austin A. J., Cammi R., Pomelli C., Ochterski J. W., Ayala P. Y., Morokuma K., Voth G. A., Salvador P., Dannenberg J. J., Zakrzewski V. G., Dapprich S., Daniels A. D., Strain M. C., Farkas O., Malick D. K., Rabuck A. D., Raghavachari K., Foresman J. B., Ortiz J. V., Cui Q., Baboul A. G., Clifford S., Cioslowski J., Stefanov B. B., Liu G., Liashenko A., Piskorz P., Komaromi I., Martin R. L., Fox D. J., Keith T., Al-Laham M. A., Peng C. Y., Nanayakkar A., Challacombe M., Gill P. M. W., Johnson B., Chen W., Wong M. W., Gonzalez C., Pople J. A., Gaussian, Inc., Pittsburgh PA, 1998.
19) Tamura *et al.*, reported[13)] that the reaction of 2,3-diphenyl-5,6-dihydropyrazine (**1a**) with diethyl fumarate gave the diethyl 3,4-diphenyl-2,5-diazabicyclo[2.2.2]oct-2-ene-7,8-dicarboxylate *via* the [4+2]-cycloaddition of the [1,5]-sigmatropic rearrangement product (**1a'**) of **1a**.
20) Yoshitake Y., Eto M., Harano K., *Heterocycles*, **45**, 1873—1878 (1997).
21) Sustmann R., Sicking W., Huisgen R., *J. Am. Chem. Soc.*, **117**, 9679—9685 (1995).

22) Matsuoka T., Hasegawa T., Eto M., Harano K., Hisano T., *J. Chem. Soc. Perkin Trans. 2*, **1993**, 1859—1865 (1993).

23) Yasuda M., Harano K., Kanematsu K., *J. Org. Chem.*, **46**, 3836—3841 (1981).

24) Hisano T., Harano K., Matsuoka T., Suzuki T., Murayama Y., *Chem. Pharm. Bull.*, **38**, 605—611 (1990).

25) Inspection of the geometries of the complexes calculated by the B3LYP/6-31G(d) method indicates that the phenyl group is rotated by 55° out of the plane of C=N bond in which the *anti* OC is less stable by 5.14 kcal/mol than the *syn* OC.

26) MOS-F (V5.0A), AM1 and PM5 calculations were performed using MOPAC2002 ver. 1.00, Fujitsu Ltd., Tokyo, Japan, 2001.

27) Ishiguro T., Matsumura M., *Yakugaku Zasshi*, **78**, 229—231 (1958).

28) Georg G. I., He P., Kant J., Wu Z., *J. Org. Chem.*, **58**, 5771—5778 (1993).

29) Taylor E. C., Makillop A., Hawks G. H., *Org. Synth.*, **52**, 36—38 (1972).

30) The compound **3ac** has been synthesized, however the NMR spectral data were not described.[13]

31) SIR92: Altomare A., Burla M.C, Camalli M., Cascarano M., Giacova-zzo C., Guagliardi A., Polidori G., *J. Appl. Cryst.*, **27**, 435 (1994).

32) teXsan: Crystal Structure Analysis Package, Version 1.11. Molecular Structure Corporation, Rigaku Coporation, 2000.